PH-DEPENDENT ABSORPTION IN THE *B* AND *Q* BANDS OF OXYHEMOGLOBIN AND CHEMICALLY MODIFIED OXYHEMOGLOBIN (BME) AT LOW CL^- CONCENTRATIONS

U. BRUNZEL, W. DREYBRODT, AND R. SCHWEITZER-STENNER
Universität Bremen, Fachbereich 1-Physik, 2800 Bremen 33. Federal Republic of Germany

ABSTRACT We have measured the optical absorbance in the maxima of the *Q* and *B* bands for oxyhemoglobin and oxyhemoglobin (BME) in dependence on the pH value of the solution in the region between pH 4.4 and pH 10. From the absorbance data optical titration curves are derived for both bands. These yield for oxyhemoglobin *pK* values 4.3, 5.3, 6.8, 7.8, and 9.0, whereas for oxyhemoglobin (BME) only one *pK* value at 4.3 is observed. These data are in good agreement to those derived recently from resonance Raman spectroscopy. The changes of the oscillator strengths in the *Q* bands are interpreted in terms of Gouterman's four-orbital model to arise from A_{1g}-distortions of the heme group, resulting from changes of the heme-apoprotein interactions due to protonation processes of amino acid-side groups in the β-chains. The difference between the sets of *pK* values in oxyhemoglobin and oxyhemoglobin BME is explained from the fact that the bifunctional reagent BME blocks important pathways of heme-apoprotein interactions. The fact that in any case increase of the *Q* band absorbance is accompanied by a corresponding increase in the *B* band absorbance leads us to the conclusion that the electronic structure of the *B* bands has to be described in terms of a six-orbital model, taking into account configurational interaction with the *L* and *N* bands.

INTRODUCTION

The investigation of the dispersion of excitation profiles and depolarization ratios of the oxidation marker line at 1,375 cm^{-1} and the spin marker line at 1,638 cm^{-1} in the Raman spectrum of oxyhemoglobin (oxyHb)[1] has recently been proven as a powerful tool to detect symmetry lowering distortions of the prosthetic heme group from its ideal D_{4h}-symmetry (Schweitzer-Stenner et al. 1984*a, b;* Schweitzer-Stenner and Dreybrodt 1985; Wedekind et al., 1985). In oxyHbA excitation profiles and depolarization ratios of both Raman lines are strongly dependent on the pH value as well as on the Cl^- concentration of the solutions. From these data by using fifth-order time-dependent perturbation theory in the framework of the electronic structure of *Q* and *B* states Schweitzer-Stenner and Dreybrodt (1985) and Wedekind et al. (1985) have deduced the relative magnitudes of static symmetry-lowering distortions in dependence on pH. They have proposed that these distortions are induced upon conformational changes of the tertiary structure of the β-chains due to protonation of amino acid side groups.

Two interpretations about the mechanism of these changes have been given. Russu et al. (1980) using NMR titration of His residues have claimed that, in contrast to the stereo-chemical model of Perutz (1970), at low Cl^- concentration the saltbridge between His146β and Asp94β should be still existing in the oxy state. Breaking of this bridge as pH changes should induce changes of tertiary structure. Recently, Perutz et al. (1985) have questioned this postulation by giving evidence that the NMR-line that was assigned to His146β by Russu et al. (1980) in reality is to be assigned to His97β. Thus, it is concluded that His97β deprotonates with a *pK* at 7.8.

The involvement of His97β is in accordance with the fact that oxyHb chemically modified by reaction with BME (bis*N*-maleimidoethyl-ether) exhibits almost no pH dependence of the excitation profiles and the depolarization ratio of both the lines at 1,375 cm^{-1} and 1,638 cm^{-1} (Wedekind et al., 1985). In BME-oxyHb the bifunctional reagent is covalently bonded between the SH group of CysF9(93β) and the imidazole of HisFG4(97β) (Simon, 1971). This first prevents the existence of the saltbridge and, secondly, imposes a constraint into the flexibility of the FG corner, thus preventing the influence of His97β titration, which is an important structural element in the cooperativity of HbA.

In a recent paper, Schweitzer-Stenner et al. (1985), by a thorough analysis of the Raman data of the two Raman lines in oxyHb at low Cl^- concentrations (<0.1 M), have

[1] *Abbreviations used in this paper:* oxyHb, oxyhemoglobin; deoxyHb, deoxyhemoglobin; HbA, human adult hemoglobin; metHb, methemoglobin; BME, bis(*N*-maleimideothyl)ether.

derived a set of pK values, which are involved in titration processes inducing distortions of the heme group. They have found values of pK to be 5.8, 6.6, and 7.8.

Using this set of pK values Schweitzer-Stenner et al. (1985) have also been able to interpret the experimental data of the rate constants for O_2-dissociation in HbA and des(His146β)HbA, as reported by Kwiatkowski and Noble 1982*a,b,* as well as those of the rate constants for CO-dissociation and association (De Young et al., 1976).

These findings prove resonant Raman scattering to be a valuable tool to obtain spectroscopic titration data on the functional groups of heme proteins.

As is well known, the absorption maxima of the B and Q bands in oxyHb and HbCO, as well as in deoxyHb, show also pH-dependent changes of the extinction coefficients (Soni and Kiesow, 1977; Fuchsmann and Appleby, 1979). From this pH dependence by using absorption difference spectroscopy, Soni and Kiesow (1977) have obtained optical titration curves of deoxyHb yielding pK values of 7.7 and 8.6. Fuchsmann and Appleby have measured titration curves of $HbAO_2$ by evaluating the absorbance differences between the Q_o and Q_v bands between pH 6 and pH 4.2. From these data they have found a pK value of 4.4. They have failed, however, to find further structure, since both Q_o and Q_v bands show increasing extinction coefficients with increasing pH. Thus, measuring the difference between both may eliminate any further structure.

In view of these data and encouraged by the evidence of the Raman data, we have measured the extinction coefficients of the B-, Q_o-, and Q_v-bands in oxyhemoglobin in dependence of pH from 4.4 to 10, because from the Raman data one expects titration processes with pK = 5.8, 6.6, and 7.8. Since these titrations induce distortions of the heme group, one can conclude that they also might change the extinction coefficients. Furthermore, also conducting these experiments in oxyHbA (BME), where the saltbridge is not present, and therefore titration processes by constraints of the FG-corner are not transferred into distortions of the heme group, one should find drastically reduced pH dependence of the extinction coefficients.

Thus, measurements of this kind can support the findings of resonant Raman scattering. Indeed we have observed complicated titration curves in all the bands of oxyHb yielding a set of five pK values at 4.3, 5.3, 6.8, 7.8, and 9, whereas oxyHb(BME) does not show any variations in all bands above pH 6.

MATERIALS AND METHODS

Human HbA was prepared from freshly drawn blood by standard procedure, as described elsewhere (Schweitzer et al., 1984*a*). The Hb-solutions were dialyzed against double distilled water at 4°C and water was renewed several times. The solution was then again centrifuged. By addition of $Na_2S_2O_4$ Hb was reduced and the deoxyHb was then equilibrated with O_2 by passage through a column of Sephadex G25 equilibrated with 10^{-3} mol buffer at pH 8. To avoid fast autooxidation, EDTA was added to the stock solution, stored in an ice bath.

To obtain BME-oxyHb, BME was added to HbO_2 in a ratio of 1 M BME to 0.5 M HbO_2 and allowed to react for 24 h at 4°C (Simon, 1971). After preparation the solution was again centrifuged. Small fractions of not fully reacted HbO_2 have no measurable influence on the experimental results. MetHb was prepared from oxyHb by addition of K_3FeCN_6 and was dialyzed against double distilled water for 24 h. Further purification was obtained by passing the metHb solution through a Sephadex G25 column.

To avoid change of inorganic ions as Cl^- we used a buffer mixed of 0.01 M citrate, 0.01 M bis-tris, 0.01 M tris, 0.01 M glycol, and 0.001 M EDTA, which shows a pH range from 4.4 to 10. pH above 5.3 was adjusted by adding NaOH; below 5.3, HCl was added. Thus, in all cases Cl^- concentration was <0.01 M, and the solutions were identical except pH. The samples for one series of measurements were prepared by diluting the stock solution in a ratio of 1:10 with the freshly adjusted buffer. The concentrations were determined by weighting the buffer and the buffer plus added stock solution to an accuracy of 0.5 mg. Thus, the concentration relative to that of the stock solution could be determined with an accuracy of 10^{-4}. Deviations in concentrations between the different samples of one experimental series could then be corrected by multiplying the absorbance values with a corresponding factor. The optical spectra were measured immediately (2 min) after mixing of the sample to avoid changes by autooxidation. The spectra were recorded in a time of 1 s.

The concentration of the samples was 15 μM given as monomer. Thus, the complete spectrum, i.e. the region of Q and B bands could be measured simultaneously with a cell of pathlength of 1 cm.

At concentrations in the μM range a significant amount of dimerization is present. It is known, however, that the optical spectra do not show any change between tetramers and dimers in oxyHb (Philo et al., 1981). The same has been observed for HbCO (Soni and Kiesow, 1977). The optical spectra were recorded with an HP8451A Diode Array Spectrometer at 20°C ± 0.5°C. The resolution of the instrument is 2 nm, the "resetability" of wavelength is 0.05 nm and the sensitivity is $5 \cdot 10^{-4}$. The time for measurement is 1 s. As a reference the corresponding buffer solution was used. The pathlength of the optical cell was 1 cm.

The spectra were stored and corrected for small concentration differences in each run of experiments. This method is prior to difference spectroscopy, since it avoids changes on the reference sample, which may introduce significant errors. Difference spectra of high quality could be obtained by subtracting the spectra with reference to the spectrum at pH 10. The final data are given in extinction coefficients at the peak maxima of the Q and B bands.

The concentration of the stock solution was determined by measuring its absorbance. Thus, different experimental series have somewhat differing concentration, but within one specific run the sample concentrations could be determined with an accuracy of 10^{-4} relative to the concentration of the stock solution.

pH values were measured using a Knick digital pH meter with an accuracy of ±0.01. Because of errors in gauging the instruments an error of ±0.05 may be realistic. The samples were adjusted in pH at steps of 0.2.

RESULTS

Fig. 1 *b* and 2 *b* show the pH-dependent absorption spectra for the OxyHb samples in the region of the Q and B bands, respectively. Small variations of a few percent are clearly visible in all three bands. To evaluate from these small changes reliable data, it is of utmost importance to know which contributions to these changes are due to deterioration of the oxidized samples with metHb, which always may be present in small amounts. Figs. 1 *a* and 2 *a* show the pH dependence of a pure metHb sample in the corresponding region. The variations are large and it might be well possible that small amounts of metHb contribute

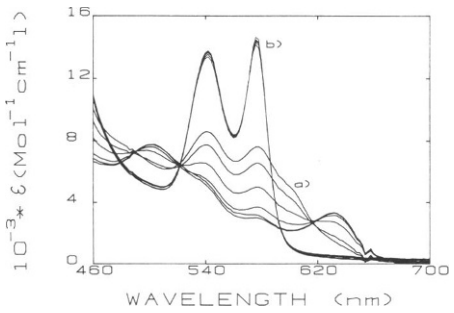

FIGURE 1 Q-band absorption spectra for metHb(a) and oxyHb(b) for various pH values. Value of pH 5 in the lowest curves rising in steps of 1 to the upper curves.

significantly to the variation measured in the oxidized samples.

Although none of the oxidized samples did exhibit any sign of metHb absorption in the metHb band at 630 nm, concentrations of a few percent might still be present. From the absorption changes of $5 \cdot 10^2$ $Mol^{-1}cm^{-1}$ 1 between pH 5 to pH 10 in the maximum of the Q_o band and the corresponding changes of the metHb extinction coefficient at the same wavelength amounting to $4.5 \cdot 10^3$ $Mol^{-1}cm^{-1}$ 1, one can compute that the presence of 1% metHb can contribute by no more than 10% to the variation observed in the oxidized sample. The same result holds for the Q_v band.

For the B band at $\lambda = 416$ nm a deterioration of 1% metHb would contribute no more than 5%. From this one would expect that the pH dependence of the Q and B bands extinction coefficients should show different behavior, if significant contributions of metHb were present. The results in Figs 3 a and 3 b, however, show that this is not the case, since all three curves can be scaled into each other within the error of measurement. Furthermore, the pH dependence is quite different from that of metHb, showing that metHb contributions are not significant. It should be noted that the data given in Figs. 3 a and b are averages of three measurements on independently prepared samples.

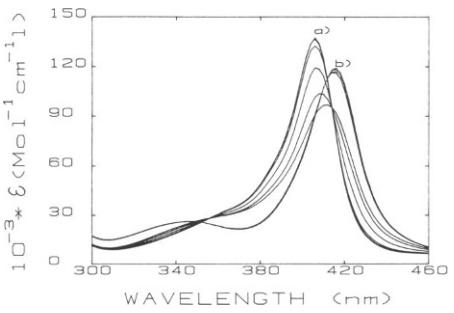

FIGURE 2 B-band absorption spectra of metHb(a) and oxyHb(b) for various pH values. For oxyHb the lowest curve is at pH 5 and rises to upper curves with steps of 1. For metHb the upmost curve is at pH 5. The lower curves are at pH values with steps of 1.

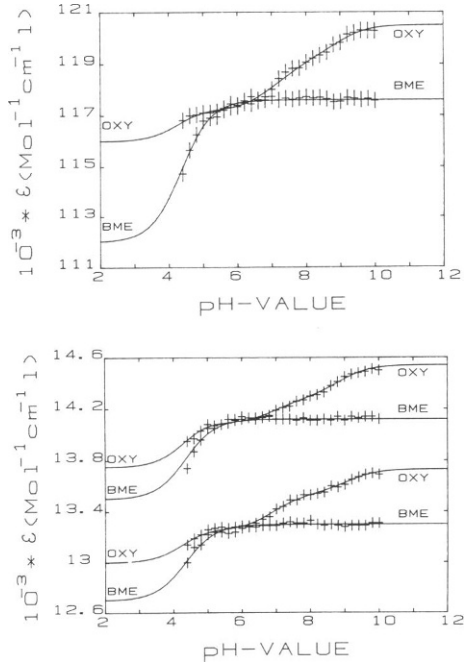

FIGURE 3 Change of extinction coefficients in the B-band (a) at 416 nm, the Q_v-band at 542 nm, and the Q_o-band (b) at 576 nm for oxyHb and oxyHb(BME). In all three cases the absorbance at 700 nm has been subtracted for baseline correction.

The results of these three runs were reproducible within the limit of error.

As a final and crucial test we have recorded the difference spectra of oxidized and pure metHb samples with respect to pH 10 by numerical subtraction over the whole spectral region. Figs. 4 a, b and 5 a, b show the results.

In the region of the Q bands the difference spectra of the oxidized samples clearly show a change of the intensity of the oxyHb Q bands. Any structure that could be related to contributions of metHb is below the level of noise. For the B band the asymmetric shape of the B band shows an increase of the oscillator strength of the band and red shift for the oxidized sample. The shape of the metHb difference spectra differs significantly from those of the oxidized sample.

From all these findings we can exclude any significant contribution of metHb above the level of noise. Furthermore, we can exclude contributions that might rise from small bands underlying the oxyHb spectra, since these contributions should also be seen in the difference spectra at the maxima of these bands in the region outside of the Q and B bands.

The situation is more complex in the case of oxyHb(BME). This modification tends to autooxidize faster than the unmodified form. The solutions of oxidized Hb(BME) therefore contained between 6 and 16% of metHb, as could be monitored from the stock solution at pH 7 from the band at 630 nm. During the time of measurement of ~2 h, the contamination of the stock

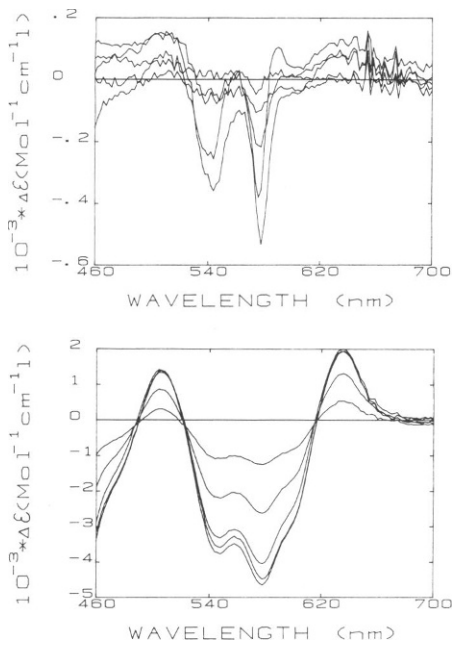

FIGURE 4 (*a*) Difference spectra of oxyHb in the region of the *Q*-bands with reference to pH 10. The amplitudes of the curves decrease with raising pH of the sample. The corresponding pH values rise in steps of 1 from pH 5 to pH 9. (*b*) Difference spectra of metHb in the region of the *Q*-bands with reference to pH 10. The amplitudes of the curves decrease with raising *pK* values, pH from 5 to 9 in steps of 1.

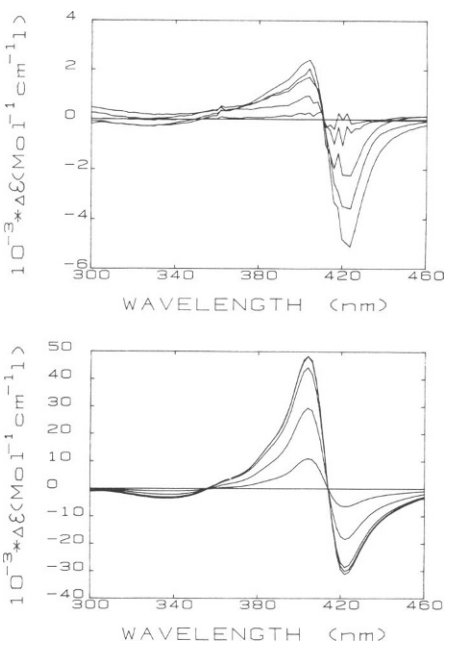

FIGURE 5 (*a*) Difference spectra of oxyHb in the region of the *B*-band with reference to pH 10. The amplitudes of the curves decrease with raising *pK* values, pH from 5 to 9 in steps of 1. (*b*) Difference spectra of metHb in the region of the *B*-band with reference to pH 10. The amplitudes of the curves decrease with raising *pK* values, pH from 5 to 9 in steps of 1.

sample stayed constant. For the correction of the raw data obtained from the oxidized Hb(BME) samples, we proceeded in the following way. The spectra were recorded 2 min after mixing the stock sample with the buffer within 1 s over the whole spectral region. From the absorbance at the 630-nm band the metHb contamination at the time of measurement was determined. Within one run the values of metHb contamination were constant within 1%, showing the largest scatter at high pH values. The reduced accuracy at higher pH values is due to the fact that the absorbance at 630 nm decreases by a factor of ~3, when going from low to high pH values. From the absorbance $A(\lambda, \text{pH})$ of the sample and the absorbance $A^{M}(\lambda, \text{pH})$ of a pure metHb sample at the same concentration the absorbance $A^{ox}(\lambda, \text{pH})$ of pure oxyHb was calculated by use of the formula

$$A^{ox}(\lambda, \text{pH}) = \frac{A(\lambda, \text{pH}) - \beta A^{M}(\lambda, \text{pH})}{1 - \beta}.$$

β is the fraction of metHb as determined from the 630-nm band.

The pH dependence of oxyHb(BME) was measured for three solutions with differing metHb contaminations between 5 and 14%. After correction the results were identical within the limits of error. They are shown by Figs. 3 *a* and 3 *b* for the *Q* and *B* bands. The data represent the average of three experiments. As in the case of oxyHb, all three bands show the same behavior. Below pH 6 the variations are larger than those in oxyHb. Above pH 6 in contrast to oxyHb there is no variation of absorbance with pH. The titration curves can all be fitted with a simple Henderson-Hasselbalck equation with *pK* 4.3. The fact that the titration curves behave opposite to those of metHb, which show large variations in the region between pH 7 and pH 10 and small ones between pH 7 and pH 4.5, is a good reference to the quality of the corrections made. If large contributions of metHb after this correction were present, one would expect variations of the corrected data in the region between pH 7 and pH 10. From this and from the identical behavior of all three bands, we conclude that the data shown are exclusively due to oxyHb(BME).

To interpret the oxyHb titration curves in terms of titration processes, we proceed in the following way. We assume that the titration processes are due to several mutually independent protonation processes, characterized by their *pK* values.

Thus, in the solution a variety of titration states *i*, *j*, *k*, *l*, *m* are present. *i*, *j*, *k*, *l*, *m* = 0,1 corresponding to protonation (1) or deprotonation (0) of the specific site. The numbers *i*, *j*, *k*, *l*, *m* are ordered with respect to rising *pK* values and we have as mass action laws

$$\frac{n_{i,j,k=0,l,m} \cdot [H^{+}]}{n_{i,j,k=1,l,m}} = K_{K}, \qquad (1)$$

where n_{ijklm} label the concentrations of the corresponding states. The occupation numbers are calculated from Eq. 1

and

$$\frac{N}{n_{i,j,k,l,m}} = \frac{\Sigma\, n_{i,j,k,l,m}}{n_{i,j,k,l,m}} \tag{1a}$$

by neglecting all terms in the sum, which give only minor contributions. They are given for the most prominent states by

$$\frac{n_{00000}}{N} = \left[1 + \frac{[H^+]}{K_1} + \frac{[H^+]}{K_2} + \frac{[H^+]^2}{K_1K_2}\right]^{-1} \tag{2}$$

$$\frac{n_{00001}}{N} = \left[1 + \left(\frac{1}{K_2} + \frac{1}{K_3} + \frac{1}{K_4}\right)[H^+] + \frac{K_1}{[H^+]} + \frac{K_1}{K_2} + \left(\frac{1}{K_2K_3} + \frac{1}{K_2K_4} + \frac{1}{K_3K_4}\right)[H^+]^2 + \frac{[H^+]^3}{K_2K_3K_4}\right]^{-1}$$

$$\frac{n_{00011}}{N} = \left[1 + \left(\frac{1}{K_3} + \frac{1}{K_4} + \frac{K_2}{K_3K_4}\right)[H^+] + \frac{K_2}{[H^+]} + \frac{K_2}{K_3} + \frac{K_2}{K_4} + \frac{[H^+]^2}{K_3K_4} + \frac{K_1}{[H^+]} + \frac{K_1K_2}{[H^+]^2}\right]^{-1}$$

$$\frac{n_{00111}}{N} = \left[1 + \left(K_2 + K_3 + \frac{K_2K_3}{K_4}\right)\cdot\frac{1}{[H^+]} + \frac{[H^+]}{K_4} + \frac{K_2}{K_4} + \frac{K_3}{K_4} + \frac{K_2K_3}{[H^+]^2} + \frac{[H^+]}{K_5} + \frac{[H^+]^2}{K_4K_5}\right]^{-1}$$

$$\frac{n_{01111}}{N} = \left[1 + \frac{K_2 + K_3 + K_4}{[H^+]} + \frac{K_2K_3 + K_2K_4 + K_3K_4}{[H^+]^2} + \frac{K_2K_3K_4}{[H^+]^3} + \frac{[H^+]}{K_5} + \frac{K_4}{K_5}\right]^{-1}$$

$$\frac{n_{11111}}{N} = \left[1 + \frac{K_4}{[H^+]} + \frac{K_5}{[H^+]} + \frac{K_4K_5}{[H^+]^2}\right]^{-1}.$$

All states with configurations, where the sites of lower pK are protonated but those of higher pK are unprotonated, show only small occupation numbers and are treated together. Their total relative occupation number is given by

$$\frac{n_R}{N} = 1 - \sum \frac{n_i}{N}, \tag{3}$$

where n_i/N are the relative occupation numbers of the species listed by Eq. 2. Fig. 6 shows the magnitudes of the relative occupation numbers for the set of pK values (4.3, 5.3, 6.8, 7.8, 9) which was finally used to fit all the experimental data for oxyHb. The lowest curve gives the small contribution due to Eq. 3.

The optical absorbance can now be calculated assuming that each configuration (i, j, k, l, m) exhibits a specific extinction coefficient A_{ijklm} by summing over the single contributions

$$A(\mathrm{pH}) = \sum A_{i,j,k,l,m} \cdot \frac{n_{i,j,k,l,m}}{N}. \tag{4}$$

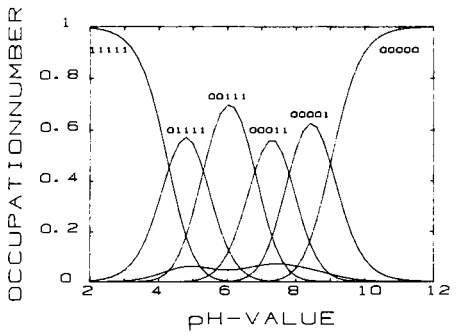

FIGURE 6 Relative occupation numbers of the different titration states as function of pH. The lowest unlabeled curve represents the occupation number n_R.

There is one restriction to the values A_{ijklm}. Since each titration state represents but a small perturbation to the heme-group, all these values must differ by only small amounts. We have simplified Eq. 4 by inserting Eq. 3 for the species with small relative populations and assuming A_{ijklm} for these configurations to be equal (A_R). This does not introduce severe errors, since their single contributions are so small that slight shifts in the corresponding A_{ijklm} are of negligible influence. Table I gives the results of A_{ijklm} for the three bands, obtained from a fitting procedure using Eq. 4 with the seven free parameters for A_{ijklm} and five free parameters for the pK values. Indeed we find all the values of A_{ijklm} to be only different by not more than a few percent as is listed in Table I.

As fitting procedure we have used a program of the CERN library called MINUITL, described by James (1972). It contains three different minimizing subroutines (SEEK, SIMPLX, and MIGRAD) for the search of a local minimum of the corresponding χ^2 function.

The fitting curves obtained from this procedure are represented by the full lines in Fig. 3. The curves of BME-Hb have been calculated by using only one pK value,

TABLE I
VALUES OF THE FITS WITH EQUATION 4 FOR THE pH DEPENDENCE OF oxyHB

	B-band	Q_v-band	Q_o-band
A_{00000}	120.5	13.73	14.54
A_{00001}	119.5	13.56	14.33
A_{00011}	118.5	13.49	14.24
A_{00111}	117.2	13.25	14.08
A_{01111}	117.2	13.25	14.1
A_{11111}	116	13.0	13.75
A_R	117.5	13.45	14.2
pK_1	9.0	9.1	8.9
pK_2	7.8	7.8	7.8
pK_3	6.8	6.8	6.8
pK_4	5.3	5.3	5.3
pK_5	4.3	4.3	4.35

Values of A are in $(\mathrm{mMol\ cm})^{-1}$.

pK = 4.3 producing two different titration states. These were the best fits obtained. All trials to obtain fits with significantly different parameters failed. From this we conclude that the fits are unique.

We have tried to fit the data using as few fitting constants as possible. Thus, at first we have neglected the pK value at pK = 9. Although the curves are well represented by this procedure at pH 8 there is a small deviation for values in the region between pH 8 and pH 9, which is beyond the error of measurement. Therefore we have included this pK value into the final fit.

The determination of the pK value pK = 5.3 is somewhat unsure, since there are only few experimental data below pH = 5.5. If one fixes the pK value at 4.3, which has been observed also by Fuchsmann and Appleby (1979) it is possible by adjusting A_{0111} to shift this value between 5.1 and 5.9. Similarly the value of pK = 4.3 is unsure by ±0.2. The accuracy of all the other pK values is in the limit of ±0.1.

DISCUSSION

In this paper we will not discuss the significance of the set of pK values to the O_2-bonding properties and Bohr effect of the molecule. This has been done by us in a recent paper (Schweitzer-Stenner et al., 1986). The important point of this work is to show that the Raman data are confirmed by measuring optical changes in the absorption bands. This is of importance, since the Raman data have to be evaluated by a rather complex mathematical formalism, whereas the absorbance changes are much more simple to interpret. The good agreement of the results gives clear evidence of the relevance of the data obtained from Raman scattering.

On the other hand the absorbance data are interesting also on their own, since they contain information about the electronic structure of the heme group. One important point is that the absorbance changes of both Q and B bands show increasing extinction constants with increasing pH.

Fig. 7 shows details of the changes of the optical absorbance in the Q_o, Q_v, and B bands. For the Q bands the position of the maxima remains unshifted within the limit of accuracy and the oscillator strengths of the bands increase with increasing pH. In the B band, however, increasing oscillator strength with pH is accompanied by a small red shift of ~1 nm.

If we assume that the changes of the band intensities are due to distortions of the heme group introduced via heme-apoprotein interaction by protonation/deprotonation processes in the protein, within the terms of Gouterman (1959) four-orbital model, only distortions of a_{1g}, b_{1g}, a_{2g}, b_{2g}-representations are of relevance. These mix the Q and B states with each other, but in the four-orbital model they do not influence other states. From this, by conservation of oscillator strength, one would expect that an increase of oscillator strength in one band should be accompanied by a decrease in the other. Furthermore, one also would expect

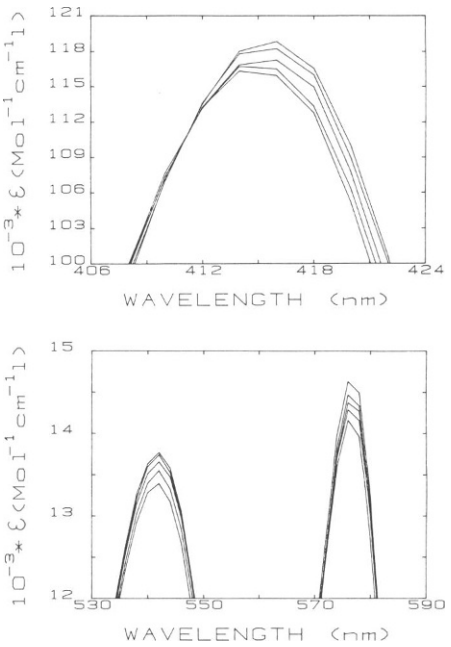

FIGURE 7 Extinction coefficient of oxyHb in the maximum of the B-band (a) and the maxima of the Q-bands (b) for various pH values. Values of pH on the lowest curve pH 5 rising in steps of 1 to the upper curves.

a blue shift of the Q-band because of the energy change of the B-band.

There is evidence, however, that the four-orbital model has to be extended, since the configurations $(a'_{2u}e_{gx})$, $(a'_{2u}e_{gy})$ $(b_{2u}e_{gx})$ and $(b_{2u}e_{gy})$, which give rise to the N and L bands, mix into the B states, whereas the Q states are reasonably well represented within the four-orbital model (Petke et al., 1978). Shelnutt (1980), in fitting Raman excitation profiles and depolarization ratio of metalloporphyrins, has provided further evidence for these findings, since he had to relax symmetry restrictions of the four-orbital models, to obtain agreement to the experimental data. Thus, the increase of intensity and red shift of the B band might well be caused by interaction with the N and L bands introduced by symmetry lowering distortions of the heme-group.

We therefore assume only the Q band to be reasonably well represented by the four-orbital model, and within this framework calculate the change of oscillator strength introduced by a_{1g}, b_{1g}, a_{2g}, and b_{2g} distortions.

O'Rourke (1983) has calculated explicitly the perturbed wave functions in $|Q^P_\pm\rangle$, and $|B^P_\pm\rangle$ frame. The results are

$$|Q^P_\pm\rangle = |Q_\pm\rangle - |B_\pm\rangle \frac{\cos 2\nu(a_{1g} \pm c_1 b_{1g} \pm c_2 b_{2g})}{E_B - E_Q} \pm |B_\pm\rangle \frac{a_{2g}}{E_B - E_Q}$$

$$|B^P_\pm\rangle = |B_\pm\rangle + |Q_\pm\rangle \frac{\cos 2\nu(a_{1g} \pm c_1 b_{1g} \pm c_2 b_{2g})}{E_B - E_Q} \pm |Q_\pm\rangle \frac{a_{2g}}{E_B - E_Q}. \quad (5)$$

The states $|B_\mp\rangle$ and $|Q_\mp\rangle$ are the states in unperturbed D_{4h}-symmetry resulting from configuration interaction. ν is the unmixing parameter, representing unmixing away from the 50:50 mixture, if the $(a_{1u}e_g)$ and $(a_{2u}e_g)$ configurations are no longer degenerate. For most metallo-prophyrins this value ranges from 0 to 9° (Shelnutt, 1984).

The entities a_{1g}, b_{1g}, a_{2g}, b_{2g} are given as matrix elements of the unmixed states B_x°, B_y°, Q_x°, and Q_y° as

$$\begin{aligned}
a_{1g} &= \langle Q_x^\circ|V_{a_{1g}}|B_x^\circ\rangle = \langle Q_y^\circ|V_{a_{1g}}|B_y^\circ\rangle \\
a'_{1g} &= \langle Q_{x,y}^\circ|V_{a1g}|Q_{x,y}^\circ\rangle = \langle B_{y,y}^\circ|V_{a1g}|B_{x,y}^\circ\rangle \\
b_{1g} &= \langle Q_x^\circ|V_{b1g}|B_x^\circ\rangle = -\langle Q_y^\circ|V_{b1g}|B_y^\circ\rangle \\
b_{2g} &= \langle Q_x^\circ|V_{b2g}|B_y^\circ\rangle = \cdot\langle Q_y^\circ|V_{b2g}|B_x^\circ\rangle \\
a_{2g} &= \langle Q_y^\circ|V_{a2g}|B_x^\circ\rangle = -\langle Q_x^\circ|V_{a2g}|B_y^\circ\rangle. \qquad (6)
\end{aligned}$$

V_Γ represents the electronic potential induced by symmetry lowering distortions of representation Γ. The values c_1 and c_2 are given in contributions of b_{1g} and b_{2g} exclusively and will not be of further interest in the discussion. Finally the energies of the perturbed states are given to first order by

$$\begin{aligned}
E_{Q_\pm}^P &= E_Q + a'_{1g} - \sin 2\nu \cdot (a_{1g} \pm c_1 b_{1g} \pm c_2 b_{2g}) \\
E_{B_\pm}^P &= E_B + a'_{1g} + \sin 2\nu \cdot (a_{1g} \pm c_1 b_{1g} \pm c_2 b_{2g}). \qquad (7)
\end{aligned}$$

From the wave functions in Eq. 5 we now calculate the dipole vectors $\langle g|\mathbf{r}|Q_\pm^P\rangle$ and $\langle g|\mathbf{r}|B_\pm^P\rangle$, where $|g\rangle$ is the ground-state of the molecule. We should keep in mind that only the vector to the Q-states is well described in terms of the four-orbital model. The vector to the B-states should be augmented by contributions from the L- and N-bands and is given only for comparison.

From the values $|\langle g|\mathbf{r}|Q_\pm^P\rangle|^2$ and $|\langle g|\mathbf{r}|B_\pm^P\rangle|^2$ we calculate the oscillator strength of the band in first order as

$$\begin{aligned}
f_Q^P &= f_Q \cdot \left(1 - 2\sqrt{\frac{E_Q f_B}{E_B f_Q}} \cdot \frac{(\cos 2\nu)\cdot a_{1g}}{E_B - E_Q}\right) \\
f_B^P &= f_B \cdot \left(1 + 2\sqrt{\frac{E_B \cdot f_Q}{E_Q \cdot f_B}} \frac{(\cos 2\nu)\cdot a_{1g}}{E_B - E_Q}\right). \qquad (8)
\end{aligned}$$

One important result is that the oscillator strengths of both bands are only changed by a_{1g} perturbations, since the b_{1g} and b_{2g} distortions only mix intensity from the Q_+ to the Q_- band and the B_+ to B_- bands, respectively. The a_{2g} perturbations contribute only in second order and are neglected. Since f_B^P, f_Q^P are within a few percent equal to f_Q and f_B, they may be taken equal and the relative change is given by the second term in the bracket. Note that within this four-orbital formulation the total oscillator strength $f_B + f_Q$ is conserved upon changes in a_{1g}.

Our experimental data show that when going in pH from 5 to 10 both Q bands change by 3%. From this we are able to estimate the magnitude of $a_{1g} \cdot \cos 2\nu$.

The oscillator strengths of the Q and B bands are $f_{Q_o} = f_{Q_v} = 0.12$ and $f_B = 1.3$ respectively (Eaton et al., 1978). $E_B = 24{,}038\ \text{cm}^{-1}$, $E_{Q_o} = 17{,}360\ \text{cm}^{-1}$ and $E_{Q_v} = 18{,}450\ \text{cm}^{-1}$. We thus obtain

$$a_{1g} \cdot \cos 2\nu = 36\ \text{cm}^{-1}; \qquad a_{1g} = 34\ \text{cm}^{-1}.$$

Thus the titration of the four groups with pK = 5.3, 6.8, 7.8, and 9.0 introduces a change of a_{1g} of $\sim 34\ \text{cm}^{-1}$, if we assume $\nu \approx 10°$.

Since the corresponding energy shift is related to sin 2ν it would amount to only 12 cm^{-1}, which cannot be resolved with an experimental set up.

The value of $a_{1g} = 34\ \text{cm}^{-1}$ results from the many interactions between the hemegroup and the protein, which change because conformational changes of the protein upon protonation processes. It is interesting to compare this value to the changes in the a_{1g} potential introduced into porphyrin upon substitution of the H atoms in positions 1 to 8 at the pyrrole rings and α to δ at the methin bridges. These have been calculated by Gouterman (1959) for substitution of alkyl from the extinction coefficients of the Q_x and Q_y bands of substituted porphyrins in relation to a model porphyrin with D_{4h} symmetry and 50:50 unmixed states.

Upon alkylation of one of the H atoms in the positions 1 to 8 the a_{1g} contribution per substitution is $a_{1g} = 30\ \text{cm}^{-1}$, alkylation of one of the positions α to δ yields $a'_{1g} = -130\ \text{cm}^{-1}$.

In comparison to this the energy change due to one protonation process is $\sim 8\ \text{cm}^{-1}$. This is $\sim 3\%$ of the value, which would result upon substitution of all H atoms in the positions 1 to 8, or 1.5% of the value resulting on substitution in the positions α to δ. A further contribution to the a_{1g} potential can arise from the interaction of the Fe^{2+} ion with the porphyrin skeleton via configurational changes in the position of the proximal histidine, which is covalently bonded to the iron. In view of this the percent numbers above have to be regarded as an upper limit.

The B band should show within the four-oribtal model a slight decrease in oscillator strength of 0.4%. In reality, however, the B band increases by 2.6%. This increase of the band has to be attributed to interactions with the L and N states, mixing into the B states.

CONCLUSION

The results can be summarized as follows: (*a*) Configurational changes of the protein structure, which are induced by protonation processes of amino side groups or rupture of saltbridges, via heme-apoprotein interactions induce distortions of the heme group. (*b*) Only distortions of a_{1g} symmetry change the oscillator strength of the Q band. This produces pH dependence of the extinction coefficients, which was measured in oxyHb and BME oxyHb. From the pH dependence of oxyHb it was found that five groups with pK = 4.3, 5.3, 6.8, 7.8, and 9 are involved. In BME-HBO_2 only one group is observed at pK = 4.4 This is in agreement to the Raman data of Wedekind et al. (1985)

and Schweitzer-Stenner et al. (1986). In BME-Hb the saltbridge between His146β-Asp94β is absent and by constraint in flexibility via the covalently bonded BME link configurational changes are not transferred to the heme group. (*c*) The experimental data of the *Q* band can be interpreted in terms of the four-orbital model. From this the a_{1g} interaction energy per protonation process is found to be of the order of 34 cm^{-1}. Within this framework the intensity of the *B* band should stay practically constant. The fact that the *B* band shows a similar increase in intensity as the *Q* bands, shows that the *B* band is not well described in the framework of the four-orbital model. (*d*) The measurements of the pH dependence of the absorbance confirm the Raman data and their theoretical interpretation.

We gratefully acknowledge many valuable discussions with Dr. D. Wedekind. We would like to thank Mrs. C. Lamm and Mrs. R. Matzullok for chemical assistance, and Mrs. C. Niemeyer for typing the manuscript. Freshly drawn blood was obtained from the "Gemeinschaftslaboratorium" of Drs. Schiwara, von Winterfeld, and Pfanzelt.

Received for publication 10 September 1985.

REFERENCES

De Young, A., R. R. Pennely, A. Tam-Wilson, and R. W. C. Noble. 1976. Kinetic studies on the binding affinity of human hemoglobin for the 4th carbon monoxide molecule. *J. Biol. Chem.* 251:6692–6698.

Eaton, W. A., K. L. Hanson, P. I. Stephens, I. C. Sutherland, I. B. R. Dunn. 1978. Optical spectra of oxy- and deoxyhemoglobin. *J. Am. Chem. Soc.* 106:4991–5002.

Fuchsmann, W. H., and C. A. Appleby. 1979. CO- and O_2-complexes of soybean leg hemoglobins: pH effects upon infrared and visible spectra. Comparisons with CO and O_2 complexes of myoglobin and hemoglobin. *Biochemistry.* 18:1309–1321.

Gouterman, M. 1959. Study of the effects of substitution on the absorption spectra of porphyrin. *J. Chem. Phys.* 30:1139–1161.

James, F. 1972. Function minimization. Proceedings of the 1972 CERN Computing and Data Processing School, Pertisau, Austria, 10–24 September, 1972. (CERN 72-21).

Kwiatkowski, L., and R. W. Noble. 1982*a*. The effect of the 146β histidine on the pH-dependence of the R-state of human hemoglobin. *In* Hemoglobin and Oxygen Binding. C. Ho, editor. MacMillan Press, Elsevier/North Holland. 403–407.

Kwiatkowski, L., and R. W. Noble. 1982*b*. The contribution of His(HC3) (146β) to the R-state Bohr-effect of human hemoglobin. *J. Biol. Chem.* 257:8891–8895.

O'Rourke, P. E. 1983. Raman excitation profiles of copper tetraphenylporphyrin in a nitrogen matrix. Ph.D. thesis, Georgia Institute of Technology.

Perutz, M. F. 1970. Stereochemistry of cooperative effects in haemoglobin. *Nature (Lond.).* 228:726–734.

Perutz, M. F., A. M. Gronenborn, G. M. Clore, J. H. Fogg, and D. T.-b. Shih. 1985. The *pK* value of two histidine residues in human haemoglobin, the Bohr effect and the dipole moments of the α—helices. *J. Mol. Biol.* 171:31–59.

Petke, I. D., G. M. Maggiora, L. L. Shipman, and R. E. Christoffersen. 1978. Stereoelectronic properties of photosynthetic and related systems: Ab initio configuration interaction calculations on the ground and lower excited singlet and triplet states of magnesium porphine and porphine. *J. Mol. Spectr.* 71:64–83.

Philo, J. S., M. L. Adams, and T. M. Schuster. 1981. Association-dependent absorption spectra of oxyhemoglobin A and its subunits. *J. Biol. Chem.* 256:7917–7924.

Russu, I., N. T. Ho, C. Ho. 1980. Nuclear magnetic resonance investigation of histidyl residues in human normal adult hemoglobin. *Biochemistry.* 21:5031–5043.

Schweitzer-Stenner, R., W. Dreybrodt, and S. el Naggar. 1984*a*. Investigation of pH-induced symmetry distortions of the prosthetic group in deoxyhaemoglobin by resonance Raman scattering. *Biophys. Struct. Mech.* 10:241–246.

Schweitzer-Stenner, R., W. Dreybrodt, D. Wedekind, and S. el Naggar. 1984*b*. Investigation of pH-induced symmetry distortions of the prosthetic group in oxyhaemoglobin by resonance Raman scattering. *Eur. Biophys. J.* 11:61–76.

Schweitzer-Stenner, R., and W. Dreybrodt. 1985. Excitation profiles and depolarization ratios of some prominent Raman lines in oxyhaemoglobin and ferrocytochrome c in the preresonant and resonant region of the Q-band. *J. Raman Spectrosc.* 16:111–123.

Schweitzer-Stenner, R., D. Wedekind, and W. Dreybrodt. 1986. Correspondence of the *pK*-values of oxyHb titration states detected by resonance Raman scattering to kinetic data of ligand dissociation and association. *Biophys. J.* 49:1077–1088.

Shelnutt, J. A. 1980. The Raman excitation spectra and absorption spectrum of a metalloporphyrin in an environment of low symmetry. *J. Chem. Phys.* 72:3948–3958.

Shelnutt, J. A. 1984. Electronic structure of metalloporphyrins and their dimers. *J. Phys. Chem.* 88:4988–4992.

Simon, S. R., D. J. Arndt, and W. H. Königsberg. 1971. Structure and functional properties of chemically modified horse hemoglobin. *J. Mol. Biol.* 58:69–77.

Soni, S. K., and L. A. Kiesow. 1977. pH-dependent Soret difference spectra of the deoxy and carbonmonoxy forms of human hemoglobin and its derivatives. *Biochemistry.* 16:1165–1170.

Wedekind, D., R. Schweitzer-Stenner, and W. Dreybrodt. 1985. Heme-Apoprotein interactions in the modified oxyhemoglobin-BME and in oxyhemoglobin at high Cl^--concentration detected by resonance Raman scattering. *Biochim. Biophys. Acta.* 830:224–232.